Article

JOURNAL OF COMPOSITE MATERIALS

Journal of Composite Materials
2014, Vol. 48(9) 1131–1137

DOI: 10.1177/0021998313482159
jcm.sagepub.com
SAGE

Fatigue and impact response of gel-coated glass mats/polyester composites

C Capela[1,2], JM Ferreira[1,3], H Cravo[2] and JM Costa[1,3]

Abstract

Composites based on polyester matrices reinforced with fiber glass mats are widely used in the automotive industry, incorporating in many cases a gel coat surface layer. This paper presents the results of a current study in polyester/short fiber glass mat composites processed by hand lay-up moulding. Different lay-up architectures were tested under impact and fatigue bending loadings. Furthermore, the influence of the gel coat surface layer on fatigue and impact loading performances was also analysed. The composites tested with gel coat layer under compression loading exhibit significant higher bending stiffness, static and fatigue strength than when the gel coat layer was under tensile loading. The impact response showed a slight variation of the peak load and on the elastic recuperation and a significant increase on maximum displacement and absorbed energy with the increase of the incident impact energy. Both energy recovery, in percentage of the incident impact energy, and residual bending strength showed a marked and almost linear decreasing with the increase of the impact energy for all loading conditions, while the absorbed energy increased with the incident impact energy, reaching about 80% of impact energy for the highest impact energies

Keywords

Glass fibers, polyester, fatigue of composites, impact tests

Introduction

Advanced composites can exhibit strong stiffness along preferential directions, good fatigue resistance and offer the flexibility and lightweight characteristics required nowadays in many constructions, like aerospace, ship building, railway structures and automotive applications. This class of materials offers flexible material solutions to the designer by allowing to optimize the strength and stiffness of a component or structure and also corrosion resistance stability and good dynamic response when compared with metal structures for similar applications. Polymer matrix composites reinforced with high-strength glass fibres are widely used in the production of structural components of high strength and low weight.[1] Polyester is an economic material that has high chemical resistance to environmental effects, high dimensional stability and low moisture absorption.

Stacking sequence optimization is one important goal to improve the stiffness and strength of laminate composites. Bezazi et al.[2,3] studied the stacking sequence effects on cross-ply laminate fatigue damage. El Mahi et al.[4] studied the influence of the stacking layer sequence (two stacking sequences $[0_7/90]_s$ and $[0_3/90/O_4]_s$ have been considered) by using finite element analysis and evaluated the loss of rigidity and energy in cross-ply laminates during tensile fatigue tests. Park et al.[5] found the optimal stacking sequence to maximize the resistance of the composite laminates by using genetic algorithms for various loading and boundary conditions.

Relatively few studies have been reported on the fatigue crack propagation in woven laminates. Mandell[6] analysed the propagation of a crack-through-thickness in notched samples loaded in tension–tension fatigue. Laminates were made of polyester resin and glass-woven plies lined up with the load

[1]CEMUC, Universidade de Coimbra, Rua Luís Reis Santos, Coimbra, Portugal
[2]Mechanical Engineering Department, ESTG, Polytechnic Institute of Leiria, Morro do Lena – Alto Vieiro, Leiria, Portugal
[3]Departament of Mechanical Engineering, Universidade de Coimbra, Rua Luís Reis Santos, Coimbra, Portugal

Corresponding author:
C Capela, Mechanical Engineering Department, ESTG, Polytechnic Institute of Leiria, Morro do Lena – Alto Vieiro, 2400-901 Leiria, Portugal.
Email: ccapela@estg.ipleiria.pt

direction. The main characteristic underlined was that the crack growth was linked to fibre tow width. Pegoretti and Ricco[7] investigated fatigue crack growth in polypropylene composites reinforced with short glass fibres. The crack growth rate level was found to decrease as the fibre weight fraction increased. A further analysis of the data indicated that crack propagation was also governed by viscoelastic creep.

Despite the excellent in-plane performance offered by laminated composites, they have relatively lower through-thickness properties. Moreover, in the case of impact loads, the resultant damage can range from matrix cracking, fibre failure and/or delaminations. This is particularly true for carbon fibre composites, due to the brittle nature of the fibre, with a consequent reduction of the residual strength.[8–12] Research studies developed in Kevlar multiaxial warp-knit fabric composites by Kang and Kim[13] showed that these materials have a high capability for absorbing impact energy while restricting the area damaged by a relatively small region compared with Kevlar woven laminates. For specific applications it can be advantageous to associate two types of fibres to form hybrid laminates[14,15] or sandwich composites.[16–18]

Functionally graded materials (FGMs) have been recently studied in mind to obtain different properties along thickness. Composite laminates can be optimized to obtain the desired properties at each layer. Sundararajan and Ganapathi[19] studied the dynamic buckling behavior of functionally graded spherical caps exposed to a thermal field using the finite-element procedure, concluding to significant influences of material gradient index on the critical buckling temperature.

The main objective of this work was to study the influence of the layer of gel coat, particularly its position on tensile or compressive side, on fatigue strength and also on impact response of a polyester matrix composite reinforced by fiber glass mat, widely used in automobile industry.

Materials and procedure

The present work studied two different lay-up composites, using polyester matrix, fiberglass mat and a gel coat layer. The two adopted architectures (3C and 4C) are composed of 2 layers of polyester matrix/fiberglass mat and a layer of gel coat (3C) or 3 layers of polyester matrix/fiberglass mat and a layer of gel coat (4C). Two fiberglass mats with 150 g/m^2 and 450 g/m^2, supplied by Taishan Fiberglass Inc. were used. Two polyester resins were used: Crystic 115 PA as matrix and Crystic 65 PA as gel coat, both supplied by Scott Bader. The accelerator used for both resins was the Butanox M-60 VRD, supplied by Azko Nobel.

The laminate was processed as follows: first, the mold was prepared, second, a uniform gel coat layer (255 g resin Crystic 65 PA and 10 g of accelerator) was applied uniformly over the mould with a roller and brush. Afterwards, 2 layers of fiber-glass mat were applied. Each layer contained 150 g/m^2 of fiber mat, 200 g of resin 115 PA and 10 g of accelerator. Finally, one last layer was placed for the case of 4C architecture. In this case, a 450 g/m^2 of fiber mat, 250 g of resin 115 PA and 10 g of accelerator was used.

Composite sheets with 400×400 mm^2 were manufactured by moulding in vacuum. Bending and impact tests were performed with gel coat in the compressed side (GCC) and with the gel coat in the tension side (GCT), as shown in Figure 1(a) and 1(b), respectively.

Specimens were cut from the composite sheet with desired dimensions. Flexural test specimens were cut to the dimensions of 80×20 mm^2 and subjected to three-point bending tests with a span of 48 mm. The thickness of the specimens was 3 mm and 2 mm for 4C and 3C architectures, respectively. Static bending tests were performed according to ASTM D638 standard, at a displacement rate of 1 mm/min, by using a Shimadzu AG-10 10 kN universal testing machine, equipped with a 1 kN load cell and TRAPEZIUM X software.

Fatigue tests were carried out at room temperature in an electromechanical machine equipped with a 5 kN load cell to monitor the load, using 60×20 mm^2 with span 48 mm. This machine allows variation of the frequency and the stress ratio of the loading wave. Constant amplitude displacement was applied with a sinusoidal wave-form at a frequency of 10 Hz and a stress ratio of $R = 0.25$. During the tests, the load and the number of cycles were recorded in a computer file. Figure 2 shows a view of the specially designed

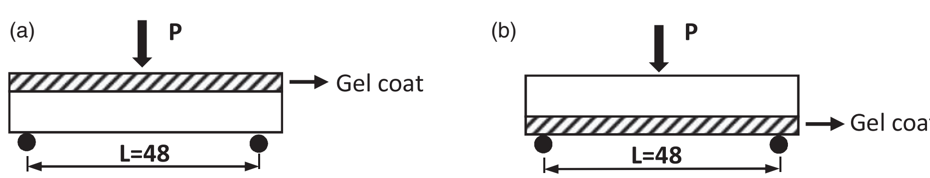

Figure 1. Test loading conditions: (a) GCC. (b) GCT. GCC: gel coat in the compressed side; GCT: with the gel coat in the tension side.

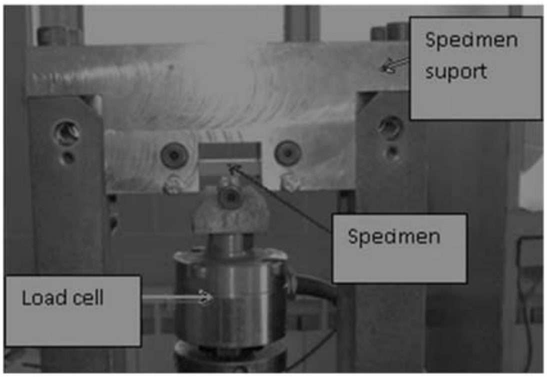

Figure 2. Fatigue testing apparatus.

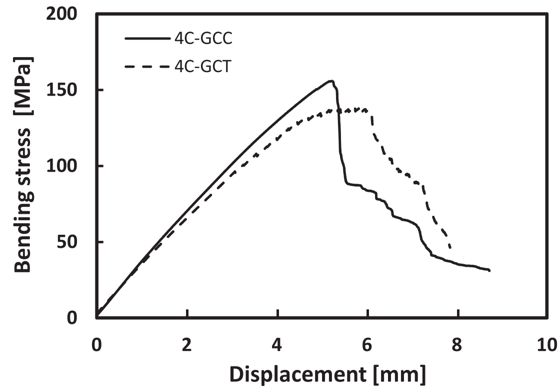

Figure 3. Typical bending stress versus displacement for 4C specimens.

three-point bending rig for the fatigue tests. All tests were carried out at room temperature. The temperature rise at the midpoint of the specimen surface was monitored for some tests, by using K-type thermocouples. A slight increase (less than 10°C) of temperature was observed.

Equation (1) was used to calculate the nominal bending stress (σ):

$$\sigma = \frac{3PL}{2bh^2} \tag{1}$$

where P is the load, L the span length, b the width and h the thickness of the specimen.

Low-velocity impact tests were performed by using a drop weight-testing machine CEAST 9350 with a semi-spherical tip impactor mass of 3.4 kg. The tests were performed accordingly to ASTM D3763 standard on square section samples of $100 \times 100\,\text{mm}^2$ supported by a circular 75 mm diameter test rigs, with the impactor stroke centred on the sample. The impactor is manufactured in steel and has 10 mm diameter then with negligible error can be considered as rigid. The impact energies used in the tests ranged from 1.5 to 8 J. These energies were previously selected in order to enable the measuring of the damaged area, but without promoting perforation of the specimens. For each condition, four specimens were tested at room temperature. After impact tests, the specimens were inspected to evaluate the position and the size of the damage. Residual strength was obtained by 3PB tests, performed in the Shimadzu AG-10 (10 kN of load capacity) universal testing machine at a displacement rate of 1 mm/min.

Results and discussion

Figure 3 shows typical curves of the nominal bending stress against the bending displacement for the particularly 4C stacking specimens. These plots are representative of the majority of the tests, showing, for both load conditions, a linear behaviour for low stresses, followed by a non-linear region, which indicates the start of the damage process, consisting of small delamination and fiber breakage. Large delamination and fiber breakage occurred at peak stress and afterwards a sudden load drop was observed. The GCC loading mode exhibits significant higher stiffness and strength and lower displacement at failure than GCT loading mode, a consequence of higher strength of tensile surface layer on GCC. Table 1 summarizes the bending strength for the composites with 3C and 4C architectures. This table indicates the average values and standard deviation obtained with three tests for each test condition. The analysis of the results shows that bending strength depends strongly on the architecture and loading mode, consequence of the different compressive and tensile strength of the fibers and gel coat. A significant increase in strength was also observed for 4C composites in comparison with 3C composites, in about 22% and 32% for GCC and GCT loadings, respectively. Bending strength under GCC loading is higher than under GCT loading, in about 64% and 52% for 3C and 4C architectures, respectively.

Table 1. Properties of laminates.

Material	Bending strength (MPa)	Fatigue strength for $N_f = 10^5$ cycles (MPa)	Fatigue ratio
3C-GCT	77.7 ± 13.2	–	–
3C-GCC	127.7 ± 12.6	–	–
4C-GCT	102.6 ± 11.9	18.4	0.18
4C-GCC	156.5 ± 10.9	41.2	0.26

Bending fatigue tests at constant displacement amplitude were performed with the electromechanical machine, where the displacement range is adjusted by a mechanical eccentric system, the median load is also mechanically adjusted by a screw system and the frequency is electronically controlled. The maximum load and minimum load were monitored at each cycle. Figure 4 shows an exemplary plot of the evolution of the normalized stress amplitude versus the normalized number of cycles, where $\Delta\sigma$ is the current stress range, $\Delta\sigma_i$ is the initial stress range, N is the current number of cycles and N_f is the number of cycles, corresponding to 25% decay in maximum stress. The composite material exhibited high stress release caused by cyclic creep. The stress release is faster and more intense for higher initial stress levels. In consequence of this stress release, the composite does not break completely, being necessary to define a failure criterion. Therefore, the number of cycles for which the maximum stress decays 25% in relation to its initial value was used as failure fatigue life.

The fatigue tests were performed only for the 4C architecture. The performance of the material in terms of fatigue strength for the two gel-coat loading positions (GCC and GCT) is compared in Figure 5, where the initial stress range is plotted against the reference failure fatigue life. In spite of a significant results scatter, the fatigue strength is reasonably fitted with a log–log straight line for both load conditions. Table 1 indicates the fatigue strength for a failure fatigue life of 10^5 cycles. Samples with the gel coat under compressive stresses (GCC) exhibit much higher fatigue strength than the composites tested with the gel coat under tensile stresses (GCT). This difference increases with failure fatigue life reaching about 125% for 105 cycles. The increased fatigue strength of GCC composites can be explained in part by higher static strength using the fatigue ratio calculated by the fatigue strength divided by the static strength. These values are indicated in Table 1, being 0.18 and 0.26 for GCT and GCC samples shows that lower fatigue strength of GCT samples is caused not only by lower static strength but also a consequence of more fatigue cracking sensibility.

Impact tests were performed by subjecting the samples to different incident impact energy levels, namely, 1.5, 2 and 3 J for 3C specimens and 5, 6 and 8 J for 4C specimens. Figure 6 shows an exemplary plot of the load versus displacement, for 4C laminates, impacted by energy of 6 J. These curves are representative of the tested stakes because in all cases plots similar to Figure 6 were obtained. These curves are characterized by an increase in the load up to a maximum value, P_{max}, followed by a load drop. The figure shows that samples tested with GCT exhibit lower P_{max}, but higher maximum displacement than specimens tested with gel coat in compression (GCC). In all tests, the impactor deforms the specimens and then always rebounds, which means that even the maximum incident impact energy was not high enough to produce full penetration. As example of this behaviour, Figure 7 shows the energy versus time curves obtained for two 4C laminates, impacted with an incident energy of 6 J.

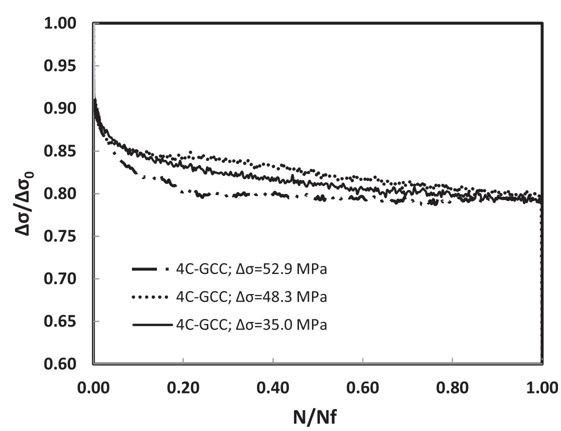

Figure 4. Exemplary curves of normalized stress amplitude versus the number of cycles.

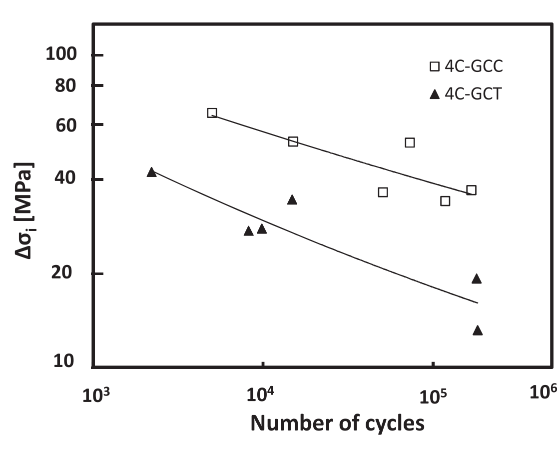

Figure 5. Fatigue S-N curves for 4C stacking sequence composites.

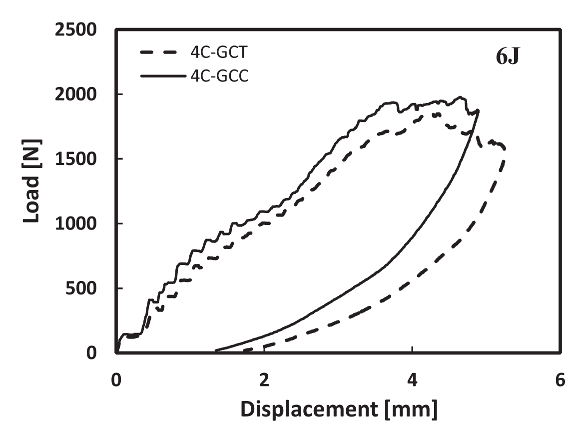

Figure 6. Load versus displacement curves for 6 J of incident impact energy.

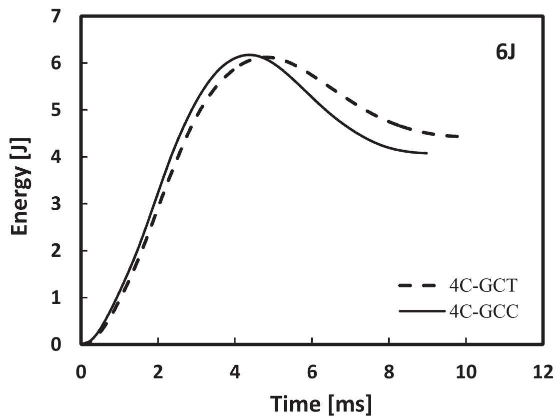

Figure 7. Energy versus time curves for 6 J of incident impact energy.

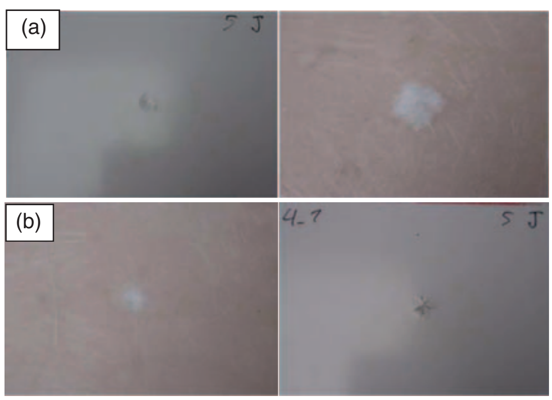

Figure 8. Images of the failure aspect: (a) 4C-GCC; (b) 4C-GCT specimen. GCC: gel coat in the compressed side; GCT: with the gel coat in the tension side.

The analysis of figure 7 shows that the elastic energy recovery is lower for specimens with gel coat in the tensile side. In fact, as shown in Figure 8, failure aspect is different between specimens with the tensile side composed by a reinforced layer or by a gel coat layer. It was observed that the damaged area in the case of gel coat layer in the tensile side shows a particular, quite different, failure pattern, forming a set of slot cracks radiating from the center of the impact zone.

Table 2 summarizes the average values of the peak load, maximum displacement, impact energy recovery and impact absorbed energy. Contrary to reported by Hosur et al.,[20] in other laminate composites, for the range of incident impact energies used in this work, an increasing of both peak load and energy recovery was not obtained with the increase of the impact energy. Anyway, peak loads obtained in laminates tested with the gel coat on the compressed side tend to be greater than the same laminates tested with the gel coat on the tensile side, particularly for 4C stacking sequence for which the difference was greater than 10%. This trend is a consequence of the lower stiffness of the gel coat layer compared with the fiber reinforced layer. Impact energy recovery shows some oscillations without a marked tendency. Their values were also calculated in terms of percentage of the impact energy and plotted against the impact energy in Figure 9. A marked and nearly linear decreasing of the percentage of recovery energy with the increasing of the impact energy was observed on the four composites/loading conditions.

Different tendencies were obtained for maximum displacement and absorbed energy. As expected, and according with reports in literature, both parameters increase significantly with the increasing of the incident impact energy. Absorbed energy, quantified in terms of percentage of the incident impact energy, is plotted against the impact energy in Figure 10. Absorbed energy is quite similar for GCC and GCT loading cases and increases significantly, and almost linearly, with the incident impact energy. It was also observed that, for the highest values of the incident impact energy, the absorbed energy reaches about 80% of impact energy, for all load cases, which indicates that a significant damage occurred.

The damaged area was calculated by using the following process: by scanning the surface of the specimens opposite the impactor contact, a corresponding closed curve to limit the visible damage of the specimen was obtained by using CometPlus5, Geomagic 12 and MeshLab v1.3.0 software; finally, the area of the previously drawn closed curve was estimated with Solidworks 2012 software. The diameter of an equivalent circle with the same area was then obtained. Figure 11 shows the diameter of the damaged area against the incident impact energy for the four different composite/loading conditions. Composites tested with gel coat in the tensile side show a significant higher damaged area than those tested with gel coat in the compressive side. In spite of the normal dispersion, the diameter of the damaged area increases almost linearly with the incident impact energy.

After impacted and scanned, the specimens were cut at a width of 60 mm and 100 mm length, containing the central damage zone. In order to obtain the residual strength, these reduced in width specimens were tested in three points, bending with the impactor contact point side in compression. Similarly to that observed with the bending strength of the non-impacted specimens, residual strength of the impacted specimens obtained for the GCC composites is quite higher than for GCT specimens: double and $\times$ 1.5 for 3C and 4C stacking sequences, respectively. As expected, the damage increases with the incident impact energy and, consequently, the residual strength decreases almost linearly in all the four test conditions.

Table 2. Average values of impact testing response.

Specimen	Impact energy (J)	P_{max} (N)	Maximum displacement (mm)	Elastic recuperation (J)	Absorbed energy (J)
3C-GCC	1.5	890.8	4.2	0.5	1.0
3C-GCC	2	813.4	5.1	0.6	1.4
3C-GCC	3	859.2	6.5	0.5	2.5
3C-GCT	1.5	796.3	4.7	0.6	0.9
3C-GCT	2	101.3	3.6	0.6	1.4
3C-GCT	3	979.9	5.0	0.7	2.4
4C-GCC	5	215.5	3.8	1.5	3.5
4C-GCC	6	2086.6	4.5	1.6	4.2
4C-GCC	8	2306.0	5.0	1.3	6.7
4C-GCT	5	1862.4	4.6	1.6	3.4
4C-GCT	6	1916.6	4.9	1.5	4.5
4C-GCT	8	2051.1	6.0	1.3	6.7

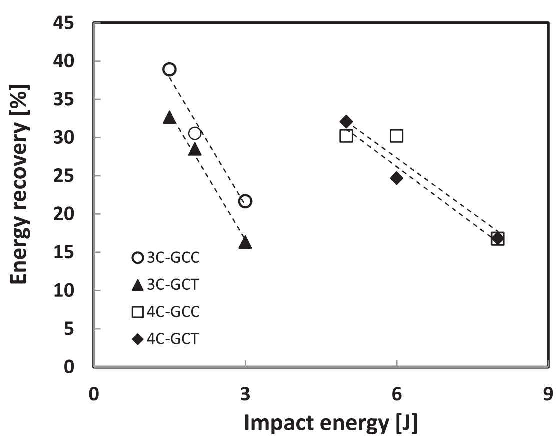

Figure 9. The effect of the impact energy and stacking sequence on elastic recuperation, in %.

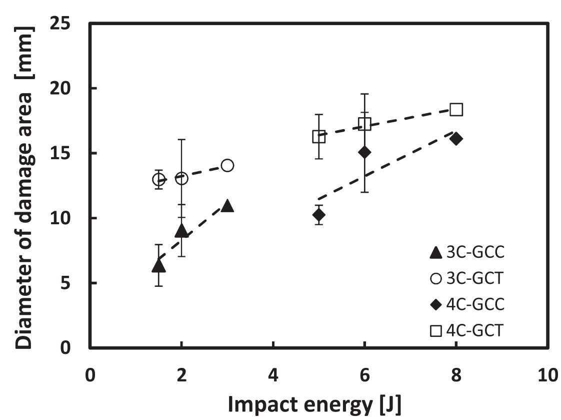

Figure 11. Damaged area in function of the incident impact energy and stacking sequence.

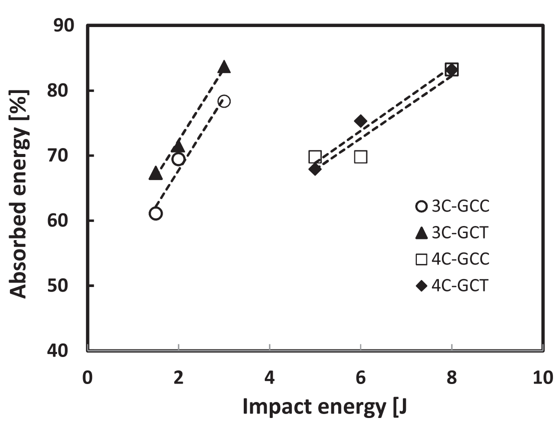

Figure 10. Effect of the impact energy and stacking sequence on absorbed energy, in %.

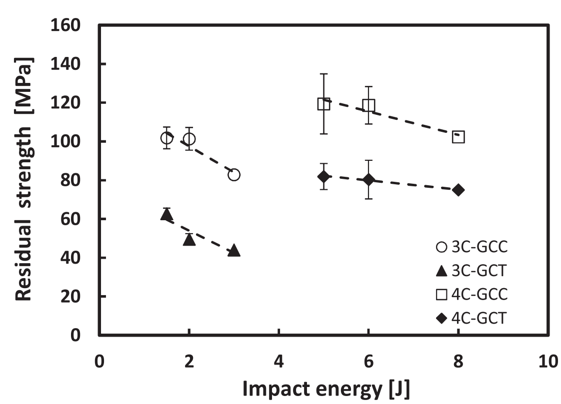

Figure 12. Residual bending strength versus incident impact energy.

Conclusions

This paper studied the effect of lay-up architecture of polyester/short fiber glass mat composites with a surface gel coat on static and fatigue behaviour under bending loading conditions as well as on the impact response. The main conclusions are

- The composites tested under GCC loading mode exhibit significant higher bending stiffness than under GCT and also a bending strength much higher than 50% for both stacking sequences. 4C composites have about 22% and 32% higher strength than 3C, respectively, for GCC and GCT loadings, but taking into account the difference of thicknesses, a slight loss of the specific strength was observed.
- Fatigue strength obtained for GCC loading is more than 125% greater than for GCT loading, which is caused by the difference on static strength and also by the different failure mechanism observed in both loading modes.
- The impact tests, using 10 mm diameter rigid impactor showed that peak load and the energy recovery did not increase significantly with the increase of impact energy. Both energy recovery, in percentage of the incident impact energy, and residual bending strength showed a marked decrease, almost linearly with the increase of the impact energy for all loading conditions. Maximum displacement and absorbed energy increase significantly with the increase of the incident impact energy. Absorbed energy, in percentage of the incident impact energy, increases almost linearly with the incident impact energy, reaching about 80% of impact energy for the highest impact energies, for all loading conditions.

Funding

This research received no specific grant from any funding agency in the public, commercial, or not-for-profit sectors.

Conflict of interest

None declared.

References

1. Pilato LA and Michno MJ. *Advanced composite materials*. Berlin, Heidelberg and New York: Springer-Verlag, 1994.
2. Bezazi A, El Mahi A, Berthelot J-M, et al. Flexural fatigue behavior of cross-ply laminates: An experimental approach. *Strength Mater* 2003; 35(2): 149–161.
3. Bezazi A, El Mahi A, Berthelot J-M, et al. Investigation of cross-ply laminates behavior in three-point bending tests. Part II: Cyclic fatigue tests. *Mat Sci* 2003; 9(1): 128–133.
4. El Mahi A, Berthelot J-M and Brillaud J. Stiffness reduction and energy release rate of cross-ply laminates during fatigue tests. *Compos Struct* 1995; 30(2): 123–130.
5. Park J-H, Hwang J-H, Lee C-S, et al. Stacking sequence of composite laminates for maximum strength using genetic algorithms. *Compos Struct* 2001; 52(2): 217–231.
6. Mandell JF. Fatigue crack propagation rates in woven and non woven fiber glass laminates. *Compos Rel ASTM STP* 1975; 580: 515–527.
7. Pegoretti A and Ricco T. Fatigue crack propagation in polypropylene reinforced with short glass fibres. *Compos Sci Technol* 1999; 59: 1055–1062.
8. Cantwell WJ and Morton J. Comparison of the low and high velocity impact response of CFRP. *Composites* 1989; 20: 545–551.
9. Prichard JC and Hogg PJ. The role of impact damage in post-impact compression testing. *Composites* 1990; 21: 503–509.
10. Davies GAO, Hitchings D and Zhou G. Impact damage and residual strengths of woven fabric glass/polyester laminates. *Compos Part A-Appl S* 1996; 27A: 1147–1156.
11. Zheng S and Sun C. Delamination Interaction in Laminated Structures. *Eng Fract Mech* 1998; 59: 225–240.
12. de Moura MFSF and Marques AT. Prediction of low velocity impact damage in carbon-epoxy laminates. *Compos Part A-Appl S* 2002; 33: 361–368.
13. Kang TJ and Kim C. Energy-absorption mechanisms in Kevlar multiaxial warp-knit fabric composites under impact loading. *Compos Sci Technol* 2000; 60: 773–784.
14. Marom G, Drukker E, Weinberg A, et al. Impact behaviour of carbon/Kevlar hybrid composites. *Composites* 1986; 17: 150–153.
15. Lee Y-S, Kang K-H and Park O. Response of hybrid laminated composite plates. *Comput Struct* 1997; 65: 965–974.
16. Gustin J, Joneson A, Mahinfalah M, et al. Low velocity impact of combination Kevlar/carbon fiber sandwich composites. *Compos Struct* 2005; 69: 396–406.
17. Salehi-Khojin A, Mahinfalaha M, Bashirzadeh R, et al. Temperature effects on Kevlar/hybrid and carbon fiber composite sandwiches under impact loading. *Compos Struct* 2007; 78: 197–206.
18. Xia F and Wu X. Work on low-velocity impact properties of foam sandwich composites with various face sheets. *J Reinf Plast Comp* 2010; 29: 1045–1054.
19. Sundararajan N and Ganapathi M. Dynamic thermal buckling of functionally graded spherical caps. *J Eng Mech* 2008; 134(2): 274–277.
20. Hosur MV, Chowdhury F and Jeelani S. Low-velocity impact response and ultrasonic NDE of woven carbon/epoxy–nanoclay nanocomposites. *J Compos Mater* 2007; 41: 2195–2212.